Astronomy & Astrophysics

Radio evolution of supernova SN 2008iz in M 82 [⋆]

N. Kimani[1], K. Sendlinger[1,2], A. Brunthaler[1], K. M. Menten[1], I. Martí-Vidal[3], C. Henkel[1,4], H. Falcke[5,6],
T. W. B. Muxlow[7], R. J. Beswick[7], and G. C. Bower[8]

[1] Max-Planck-Institut für Radioastronomie, Auf dem Hügel 69, 53121 Bonn, Germany
   e-mail: nkimani@mpifr-bonn.mpg.de
[2] Argelander-Institut für Astronomie, Auf dem Hügel 71, 53121 Bonn, Germany
[3] Onsala Space Observatory, Chalmers Univ. of Technology, 43992 Onsala, Sweden
[4] Astron. Dept., King Abdulaziz University, PO Box 80203, 21589 Jeddah Saudi Arabia
[5] Department of Astrophysics, Radboud University Nijmegen, Postbus 9010, 6500 GL Nijmegen, The Netherlands
[6] ASTRON, Postbus 2, 7990 AA Dwingeloo, The Netherlands
[7] Jodrell Bank Centre for Astrophysics, School of Physics and Astronomy, The university of Manchester, Oxford Road,
   Manchester M13 9PL, UK
[8] Academia Sinica Institute of Astronomy and Astrophysics, 645 N. Aóhoku Place, Hilo, HI 96720, USA

ABSTRACT

We report on multi-frequency Very Large Array (VLA) and Very Long Baseline Interferometry (VLBI) radio observations for a monitoring campaign of supernova SN 2008iz in the nearby irregular galaxy M 82. We fit two models to the data, a simple time power-law, $S \propto t^\beta$, and a simplified Weiler model, yielding decline indices of $\beta = -1.22 \pm 0.07$ (days 100−1500) and -1.41 ± 0.02 (days 76−2167), respectively. The late-time radio light-curve evolution shows flux-density flares at ∼970 and ∼1400 days that are a factor of ∼2 and ∼4 higher than the expected flux, respectively. The later flare, except for being brighter, does not show signs of decline at least from results examined so far (2014 January 23; day 2167). We derive the spectral index, α, $S \propto \nu^\alpha$ for frequencies 1.4 to 43 GHz for SN 2008iz during the period from ∼430 to 2167 days after the supernova explosion. The value of α shows no signs of evolution and remains steep ≈−1 throughout the period, unlike that of SN 1993J, which started flattening at ∼day 970. From the 4.8 and 8.4 GHz VLBI images, the supernova expansion is seen to start with a shell-like structure that becomes increasingly more asymmetric, then breaks up in the later epochs, with bright structures dominating the southern part of the ring. This structural evolution differs significantly from SN 1993J, which remains circularly symmetric over 4000 days after the explosion. The VLBI 4.8 and 8.4 GHz images are used to derive a deceleration index, m, for SN 2008iz, of 0.86 ± 0.02, and the average expansion velocity between days 73 and 1400 as $(12.1 \pm 0.2) \times 10^3$ km s^{-1}. From the energy equipartition between magnetic field and particles, we estimate the minimum total energy in relativistic particles and the magnetic fields during the supernova expansion and also find the magnetic field amplification factor for SN 2008iz to be in the range of 55−400.

Key words. radio continuum: galaxies – galaxies: individual: M 82 – supernovae: individual: SN 2008iz

1. Introduction

Radio-loud supernovae are rare events of which just a few dozen have been detected so far (Weiler et al. 2002). Most of them are relatively distant or fairly weak, making them difficult to study in great detail. To date, the best-known example is SN 1993J in M 81 (Martí-Vidal et al. 2011a,b and references therein), which has been studied extensively because of its proximity (3.63 Mpc, Freedman et al. 1994), environment (which allows for multi-wavelength studies), and galaxy orientation (M 81 is seen almost face-on). The discovery of SN 2008iz (Brunthaler et al. 2009a) offers the possibility of studying another supernova at a very similar distance in great detail and to make a comparison to SN 1993J. For instance, considering the peak 5 GHz radio luminosities, SN 2008iz at $L_{5\,\text{GHz}} \propto 24.4 \times 10^{26}$ erg^{-1} Hz^{-1} is comparable to SN 1993J at $L_{5\,\text{GHz}} \propto 15.5 \times 10^{26}$ erg^{-1} Hz^{-1} (van Dyk et al. 1994). The two supernovae are also comparable in the time they took to reach their peak after the explosion,

with SN 2008iz taking ≈125 days, while SN 1993J took 133 days (Weiler et al. 2007).

Supernova 2008iz was discovered in M 82, which is a nearby irregular (IO) galaxy forming part of the M 81 group. This galaxy harbours numerous bright radio supernova remnants with the current estimate at 50 supernovae (Muxlow et al. 1994; Beswick et al. 2006; Fenech et al. 2008; Kronberg et al. 2000; Weiler et al. 2002).

Supernova 2008iz was discovered in 2009 April as a bright radio transient (Brunthaler et al. 2009a,b). The explosion date of the supernova is estimated to be 2008 February 18 ± 6 days (Brunthaler et al. 2009b; Marchili et al. 2010). The discovery was made at radio wavelengths with the Very Large Array (VLA) at 22 GHz (Brunthaler et al. 2009a) and confirmed with MERLIN (Muxlow et al. 2009; Beswick et al. 2009) and the Urumqi 25-m telescope at 5 GHz (Marchili et al. 2010). Endeavours to make detections in other astronomical windows have never been successful. For instance, there are no detections in visible light and the X-ray regimes (Brunthaler et al. 2009b). Varenius et al. (2015) also reported the Low-Frequency Array for Radio Astronomy (LOFAR) non-detection at 154 MHz.

However, a detection of the near-IR counterpart for SN 2008iz at ~480 days was reported by Mattila et al. (2013) after careful analyses using image-subtraction techniques and considering possible uncertainties caused by the differing filter response functions between the Gemini-North telescope and the *Hubble* Space Telescope. Overall, this makes it challenging to classify this supernova. However, since no type Ia supernova has yet been detected in the radio regime in M 82 (Pérez-Torres et al. 2014), we can firmly say that SN 2008iz is a core-collapse supernova, in agreement with both Brunthaler et al. (2009b) and Mattila et al. (2013).

The position of SN 2008iz is estimated to be $\alpha_{\rm J2000} = 09^{\rm h}55^{\rm m}51\fs551 \pm 0\fs008$, $\delta_{\rm J2000} = +69°40'45\farcs792 \pm 0\farcs005$ (Brunthaler et al. 2009b), which is 2.5″ (43 pc) south-west of the photometric centre of M 82 based on the 2.2 μm peak (Weiß et al. 2001). The location of the supernova is heavily obscured by dust and gas, hiding the region from direct observations at optical wavelengths (Weiß et al. 2001). Brunthaler et al. (2010) estimated the extinction towards SN 2008iz to be $A_v \sim 24.4$ mag, concluding that the reason for the supernova non-detections was that it exploded behind a large dusty interstellar cloud. However, using the same data and relations, Mattila et al. (2013) obtained a total extinction of ~48.9 mag, suggesting that the authors may have omitted multiplying the value of $N(\rm H_2)$ by 2 to convert to hydrogen nuclei before applying the extinction relation of Güver & Özel (2009). The near-IR detection could indicate that the supernova was located in the foreground with most of the $\rm H_2$ column density behind the site of SN 2008iz (Mattila et al. 2013).

Very Long Baseline Interferometry (VLBI) observations reveal the expansion of SN 2008iz to be self-similar with an expansion velocity of $\approx 21\,000$ km s^{-1} over the first 430 days after the explosion, making it one of the fastest expanding radio supernovae, with an expansion index, m, of 0.89 ± 0.03 (Brunthaler et al. 2010). The modelled light curve by Marchili et al. (2010) showed that synchrotron self-absorption (SSA) is negligible, making free-free absorption (FFA) the most significant process during the supernova expansion.

Radio monitoring of SN 2008iz with VLA and VLBI has been ongoing on a regular basis since its discovery. We describe the monitoring and data reduction process in Sect. 2. In Sect. 3 we present multi-frequency radio observations from 36 to 2167 days after the explosion. In Sect. 4 we discuss the variations in the spectral index α, equipartition minimum energy and magnetic fields, and the evolution of the magnetic field evolution $B_{\rm eq}$ and its amplification. We present our summary in Sect. 5.

2. Observations and data calibration

The radio monitoring campaign conducted with the VLA at 1.4, 4.8, 8.4, 22, and 43 GHz to trace the evolution of the radio emission from SN 2008iz has been ongoing since the discovery of the emission in 2008. The first series of observations is archival and corresponds to the data published by (Brunthaler et al. 2009b, 2010). It consists of six observations (epochs 1−6 in Table A.1) obtained between 2008 March 24 (day 36) and 2009 September 19 (day 580). For details on the observations of these epochs, we refer to the respective publications. For the later observations, the data were taken in the standard continuum observation mode with a total bandwidth of 128 MHz, each in dual circular polarisation. During these epochs, observations were made in VLA configurations A, AB, B, and C. Flux density measurements were derived using calibrator 3C 48. The flux calibrator was observed for a total time of two minutes in each observation. The

observation used a switching cycle of six minutes, spending on average one minute on the phase calibrator J1048+7143 and five minutes on M 82. The cycles were repeated five times over the observations, yielding an integration time of ~25 min on M 82 at each frequency.

The last epoch of VLA observations on 2014 January 23 was obtained during a confirmation search of a newly discovered Type Ia supernova, SN 2014j at C and K bands under the observation code TOBS0008 at configuration AB. Data were taken in the standard continuum observation mode with a total bandwidth of 128 MHz, each in dual circular polarisation. The flux calibrator 3C 48 was observed for a total time of three minutes. The observation used a switching cycle of nine minutes, spending an average time of 30 s on the phase calibrator J1048+7143 and eight minutes on M 82. The cycle was repeated four times over the observation, yielding an integration time of ~32 min on M 82 at both frequencies.

The VLA observations in this work are matched by high-resolution VLBI observations at 1.6, 4.8, and 8.4 GHz. These were taken with a network consisting of the Very Long Baseline Array (VLBA), the Green Bank 100-m telescope, and the Effelsberg 100-meter telescope, leading to a maximum resolution of 4.3 milliarcsec (mas) at 1.6 GHz, 1.2 mas at 4.8 GHz, and 0.8 mas at 8.4 GHz. SN 2008iz was observed 15 times between 2009 October and 2013 January in dual polarisation. The total bandwidth of most datasets is 64 MHz, although two datasets have a bandwidth of 32 MHz and three have a bandwidth 260 MHz wide. The fluxes were calibrated using system temperature measurements and standard gain curves, and the AGN in M 81 (M 81*) was used as a phase reference calibrator. The calibrator J1048+7143 was observed several times during each observation run, each time for 90 to 120 s. SN 2008iz and M 81* were observed in turns for 45 to 55 s at 1.6 GHz and ~80 s at 4.8, and 8.4 GHz during each observation run.

The VLA and VLBI data were reduced using standard packages within the AIPS (Astronomical Image Processing Software) of the National Radio Astronomy Observatory (NRAO). To ascertain the late-time enhancement of flux values, which are much higher than expected from the supernova radio light curve, the VLA data was run using "CASA-EVLA_pipeline1.1.3" of NRAO for all epochs after 2009 September 19. The results from both data reduction procedures agree.

3. Results

Tables A.1 and A.2 contain the complete VLA and VLBI logs of radio flux measurements of SN 2008iz. The first column in each table lists the observation dates. The second column lists the number of days elapsed since explosion, which is estimated to be 2008 February 18 (±6) (Marchili et al. 2010), while the remaining columns list the integrated or peak flux density or the source size at different frequencies. To minimise the contribution of the diffuse emission in M 82 to the supernova measurements, we used only baselines longer than 30 kλ in the imaging. The AIPS task "JMFIT" was used to determine the flux by fitting a 2D Gaussian to the identified compact supernova source. The flux errors of the VLA observations were derived by adding in quadrature the formal errors from the 2D Gaussian, a 5% systematic error, and a small random error derived as the difference between peak and integrated flux densities. The errors of the VLBI 1.6 GHz fluxes were derived in a similar way; adding in quadrature the formal errors from 2D Gaussian fit to the sources, and a 9% systematic error. However, the supernova is resolved at 4.8 and 8.4 GHZ in the VLBI data, thus their integrated fluxes

cannot be derived in the same way as for the other observations. In Table A.2 we list the peak intensities at 4.8 and 8.4 GHz.

3.1. Light curve

The light curve of SN 2008iz is well fit by a power law of the form

$$S = K_0 \left(\frac{t - t_0}{1\,\text{day}}\right)^{\beta}, \tag{1}$$

especially in the well-sampled optically thin regime, that is, 5 and 22 GHz (see Fig. 1). K_0 is a flux scaling factor that does not change the overall behaviour of the fit, $(t - t_0)$ is the time elapsed after the explosion date, while β is the flux decay index. The obtained fit results (see Fig. 1) with β and K_0 as free parameters at 5 GHz (100–1500 days) are $K_{0\,5\,\text{GHz}} = (6.29 \pm 2.22) \times 10^4$ mJy and $\beta = -1.22 \pm 0.07$. The time range 0–100 days was excluded because the radio emission from the supernova shock wave was still within the optically thick regime, while the last epochs of the data sets have their peak intensity higher than expected from the light curve. The obtained fit value at 22 GHz (50–1500 days) with both β and K_0 as free parameters yields $K_{0\,22\,\text{GHz}} = (1.46 \pm 0.33) \times 10^4$ mJy and $\beta = -1.18 \pm 0.05$. Considering the 5 GHz data set, which is better sampled over the time range than the one at 22 GHz, we adopted a β value of -1.22 ± 0.07 to be more representative. Fitting the 22 GHz data with our adopted β value, we obtain the scaling parameter $K_{0\,22\,\text{GHz}}$ to be $(1.73 \pm 0.10) \times 10^4$ mJy. A fit to all frequencies (Fig. 3) using one single β value of -1.22 ± 0.07 yields a different K_0 value for each frequency. The values of K_0 are $K_{0\,1.4\,\text{GHz}} = (1.19 \pm 0.60) \times 10^5$ mJy, $K_{0\,5\,\text{GHz}} = (6.19 \pm 0.17) \times 10^4$ mJy, $K_{0\,8.4\,\text{GHz}} = (3.57 \pm 0.40) \times 10^4$ mJy, $K_{0\,22\,\text{GHz}} = (1.73 \pm 0.1) \times 10^4$ mJy, and $K_{0\,43\,\text{GHz}} = (3.77 \pm 0.52) \times 10^3$ mJy. The derived scaling factor K_0 yields a normalised average spectrum that depends on frequency, as shown in Fig. 2.

Although the simple power-law (see Eq. (1)) describes the optically thin regime of the light curve very well, a complete fit to the supernova light-curve model is not possible because we have data for only very few epochs in the optically thick regime. For the complete radio light curve, we fit the simplified Weiler model (Weiler et al. 2007) described as

$$S_{(\nu)} = K_1 \left(\frac{\nu}{5\,\text{GHz}}\right)^{\alpha} \left(\frac{t - t_0}{1\,\text{day}}\right)^{\beta} e^{-\tau}, \tag{2}$$

where K_1 is a scaling factor in Jy and α is the spectral index of the emission in the optically thin regime. The exponent β is related to the flux density drop at late epochs, normally affected by both the spectral index, α, and the opacity, τ. The date of explosion is denoted as t_0, and t is the epoch of observation. The opacity of thermal electrons of the circumstellar medium (CSM) in Eq. (2) is modelled as

$$\tau = K_2 \left(\frac{\nu}{5\,\text{GHz}}\right)^{-2.1} \left(\frac{t - t_0}{1\,\text{day}}\right)^{\delta}, \tag{3}$$

where K_2 is the scaling factor and δ is the absorption decline index related to the CSM radial density profile derived as $\delta = \alpha - \beta - 3$. The exponent -2.1 corresponds to the spectral dependence of FFA by thermal ionised gas in the radio regime.

To constrain the simplified Weiler model, we applied the best-fit parameters of models 2 and 3 obtained by (Marchili et al. 2010) at 5 GHz (i.e. $K_1 = (2.14 \pm 0.04) \times 10^5$ mJy, $\beta = -1.43 \pm 0.05$, $t_0 =$ 18 Feb. 2008, $K_2 = (11.0 \pm 0.7) \times 10^4$ mJy,
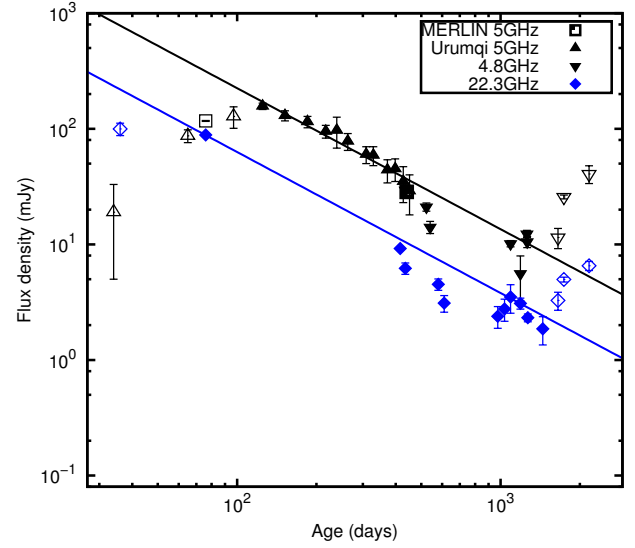

Fig. 1. Fits to the light curve of the optically thin regime of SN 2008iz at 5 and 22 GHz. β and K_0 (see Eq. (1)) are derived from the fit to the data over the range of 100–1500 days for 5 GHz and 60–1500 days for 22 GHz. The fitted data are shown as filled symbols, while the data not used to fit are shown as open symbols. The MERLIN 5 GHz data were taken from Beswick et al. (2009) and the Urumqi 5 GHz from Marchili et al. (2010). The remaining data are tabulated in Table A.1.
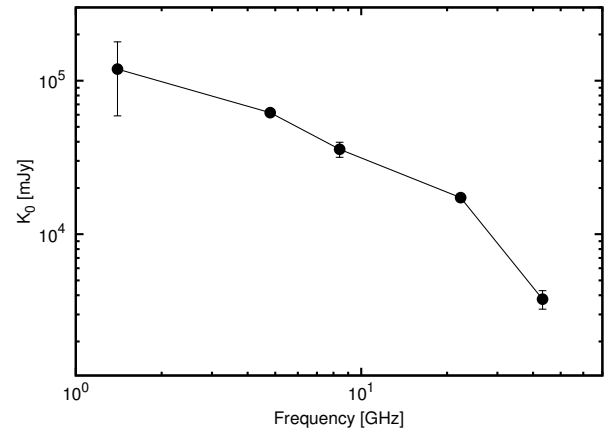

Fig. 2. Normalised average spectrum of the variation of K_O with frequency for the optically thin power-law model.

$\delta = -2.65 \pm 0.10$), and from (Brunthaler et al. 2010) we obtained the spectral index, $\alpha = -1.08 \pm 0.08$. We fit all frequencies at the same time, as shown in Fig. 4, using β as a free parameter, for which a value of $\beta = -1.41 \pm 0.02$ was determined.

The model satisfactorily fits the flux density decline from day 500 except for the 1.4 GHz observations, which fall well below the model fit in Fig. 4. The lower flux densities at 1.4 GHz are also confirmed by a 3σ LOFAR non-detection limit of SN 2008iz at a level of 0.41 mJy/beam at the even lower frequency of 154 MHz (Varenius et al. 2015). Plausible explanations might be FFA from a dense foreground screen along the line of sight. Other effects, such as a low-frequency cut-off caused by a Razin-Tsytovich effect, might also help explain the lower 1.4 GHz flux and LOFAR non-detection. From the same figure, the observations at 43.2 GHz drop quite fast past ∼1000 days. This drop is most likely related to synchrotron ageing of the emitting electrons in the shocked CSM.
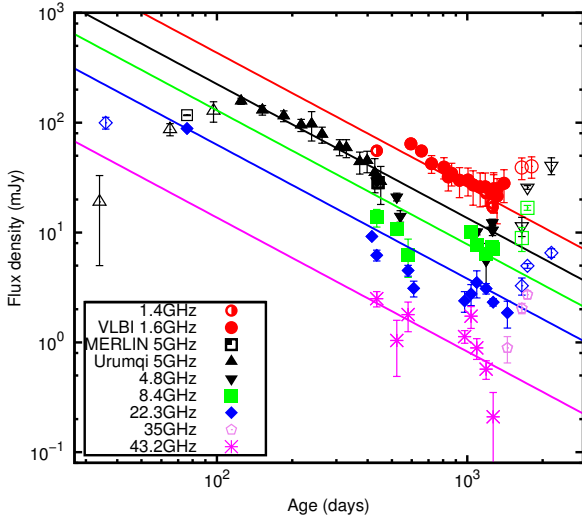
Fig. 3. Combined multi-frequency light curve for the optically thin regime of SN 2008iz. The fitted data are shown as filled symbols, while the data not used to fit are shown as open symbols. The data sources are indicated in Fig. 1, while the 1.6 GHz VLBI data are tabulated in Table A.2. The lines represent simple power-law fits to the data at the different frequencies as colour coded in the legend.
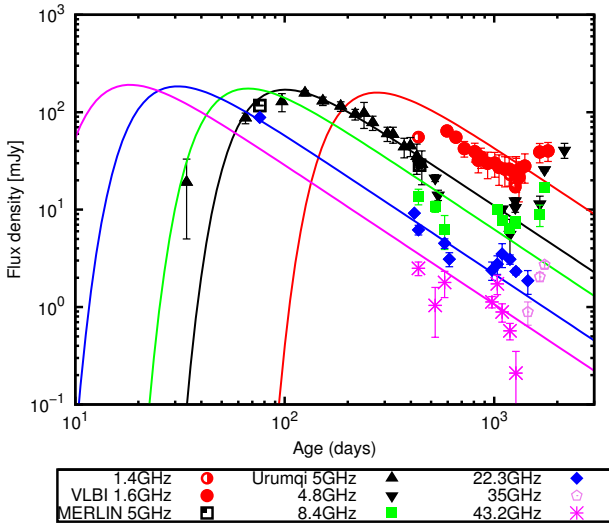

Fig. 4. Multi-frequency light curve of SN 2008iz. The MERLIN 5 GHz data were taken from Beswick et al. (2009) and the Urumqi 5 GHz from Marchili et al. (2010). The remaining data are tabulated in Tables A.1 and A.2. The black line represents a Weiler model fit to 5 GHz data obtained by Marchili et al. (2010) with the Urumqi telescope. The other lines represent light curves calculated using the equations in the text for the other frequency data sets as colour coded in the legend.

3.2. Deceleration of SN 2008iz

The VLBI images of SN 2008iz at 4.8 and 8.4 GHz are shown in Figs. 6 and 7, respectively. All the images are phase referenced to the M 81 core, M 81*, for consistency in their alignment. The SNR is resolved at these frequencies. We used natural weighting to reveal more information on the larger-scale structures. The size and shape of the beam used to restore the images was determined by the set of antennas (uv-coverage) that were employed for each of the considered data sets. For instance, the resolution of the images in Figs. 6e, f, and 7e and h is lower because some
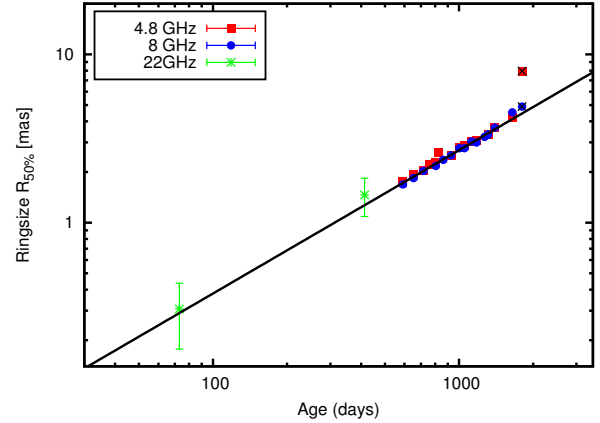
Fig. 5. Expansion curve of SN 2008iz. The two data points at 22 GHz were taken from Brunthaler et al. (2010), while the last two data points (overlaid with a black ×) were excluded from the fit.

telescopes, especially the Effelsberg 100 m telescope, did not take part in the observations.

The images show that the supernova expansion started with a shell-like structure that became increasingly more asymmetric. Overall, we see expansion with similar velocities in all directions. During the later epochs, the emission distribution breaks up and shows substructures in the southern part of the ring. There, the ring is much brighter than in its other parts, indicating a denser surrounding medium along the southern direction.

The deceleration of SN 2008iz is derived from the VLBI images convolved with a dynamic beam at 4.8 and 8.4 GHz. A dynamic beam (see Marcaide et al. 1997) scales the resolution of the later epochs to the resolution of the first epoch with respect to the size of the supernova shell size before imaging. It eliminates the systematic errors that would otherwise arise from the different resolution with which the SNR was imaged while it expanded. We obtained the size of the SNR with the AIPS task "IRING", which was used to fit 2D Gaussians to the obtained light profiles. The centre of the SNR remains at the same position during the time span of our observations. We took the radius of the supernova ring to lie at 50% of the peak intensity on the outside of the bright rim since this is the real ring size times an unknown factor. This method is more reliable than taking the maximum of the ring as the radius (see a more detailed description in Brunthaler et al. 2010; Beswick et al. 2006). We fit a power law of the form

$$R_{50\%} = c_y(t - t_0)^m \tag{4}$$

to the size evolution of SN 2008iz, where c_y is a scaling factor, $(t-t_0)$ is the time elapsed after the explosion date, and m is the deceleration index. We derive values of $c_y = (7.5 \pm 0.9) \times 10^{-6}$ arcsec/day and $m = 0.86 \pm 0.02$. The errors are obtained from the post-fit covariance matrix. The size evolution and deceleration of SN 2008iz are displayed in Fig. 5. We also show two 22 GHz data points from Brunthaler et al. (2010) that were included in the analysis. The last two data points were excluded from the fit since we know from the light curve that there is a change in the surrounding medium of SN 2008iz at around 1400 days after the explosion that is not caused by internal processes.
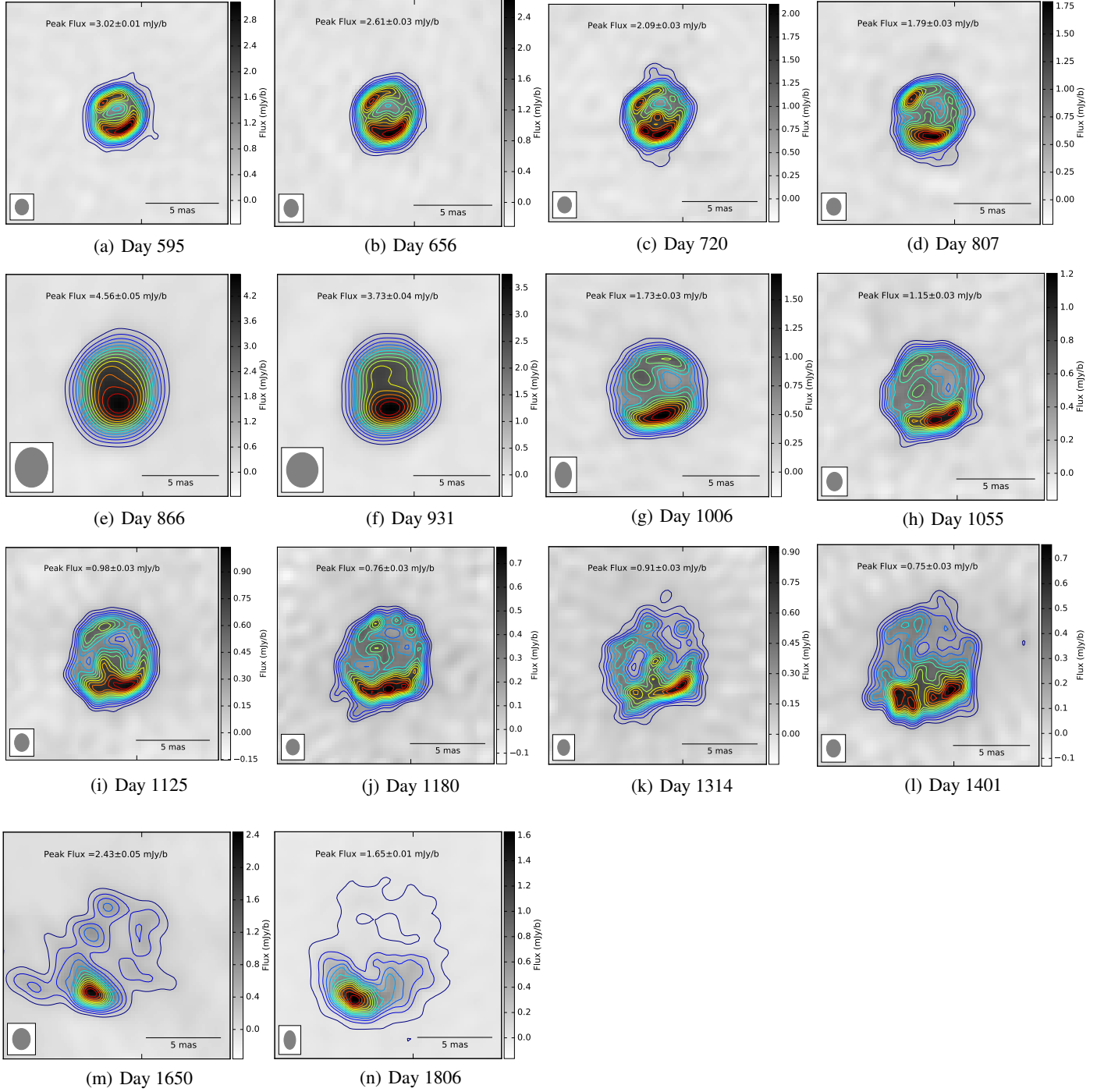
Fig. 6. Natural weighted VLBI images of the expanding shell produced by supernova SN 2008iz at 4.8 GHz. They cover the observation periods between 2009 October and 2013 January as summarized in Table A.2. The figures show the 4.8 GHz linear grey-scale images overlaid with their contour maps that scale to the peak intensity at each epoch (listed in each panel). All image contours correspond to 6% of the peak intensity (lowest contour) and subsequent increases by 6%. The images have been convolved with the natural weighting beam, shown in the bottom left corner of each panel.

4. Discussion

4.1. Flux-density flare from day ~970

A zoom into the light curve at the higher frequencies (see Fig. 8) uncovers excess emission from the supernova after $t = 970$ days and after $t = 1400$ days. We note that the extra emission after $t = 970$ days is detected at 8.4, 22.3, and 43.2 GHz, while the enhancement at $t = 1400$ days is detected at 4.8, 8.4, 22, and

35 GHz. The later flare after time ≥ 1400 days is also confirmed with our densely sampled VLBI 1.6 GHz results. The extra emission increases the total flux density of the supernova by a factor of ~2 at $t = 970$ days, lasting for about 240 days. The second flare increases the total flux density by a factor of ~4, without showing signs of flux decline so far, that is, in 2014 January. This calls for a continuation of the monitoring to determine how long the second flare lasts.
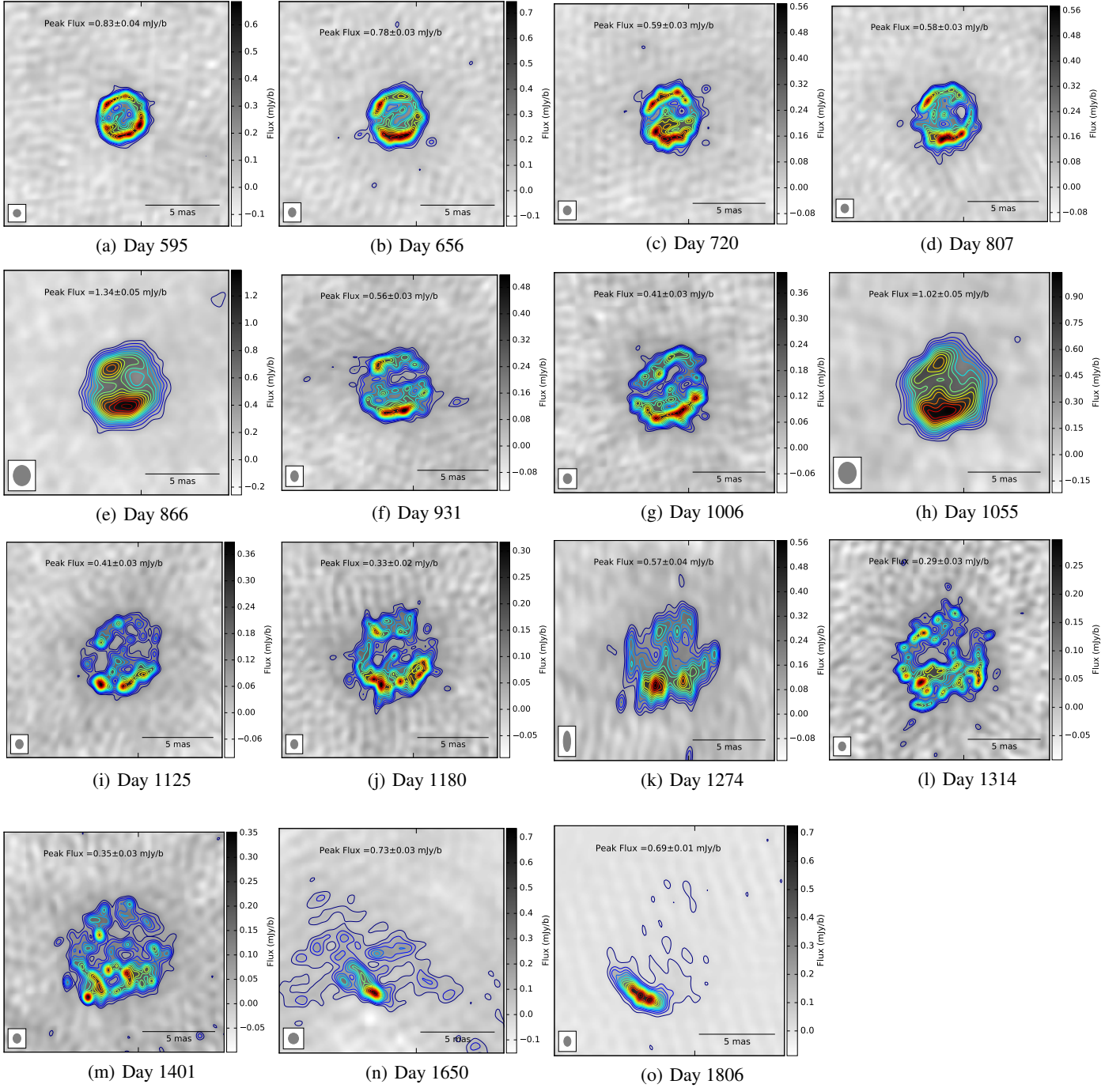
Fig. 7. Natural weighted VLBI images of the expanding shell produced by supernova SN 2008iz at 8.4 GHz. They cover the observation periods between 2009 October and 2013 January as summarized in Table A.2. The figures show the 8.4 GHz linear grey-scale images overlaid with their contour maps that scale to the peak intensity at each epoch (listed in each panel). All image contours correspond to 6% of the peak intensity (lowest contour) and subsequent increases by 6%. The images have been convolved with the natural weighting beam, shown in *the bottom left corner of each panel.*

The source is obviously optically thin at all frequencies during the flares, and its spectral index remains steep (see Sect. 4.2). Weiler et al. (2002) indicated that a supernova whose radio emission preserves its spectral index while deviating from the standard model shows evidence of a change in the conditions of the CSM that its remnant expands into. We therefore examined the changes in the density of the CSM as the explanation to the observed flares. According to Chevalier (1982), radio luminosity is related to the average CSM density ($\rho_{csm} \propto \dot{M}/w$) through

$$L \propto \left(\frac{\dot{M}}{w}\right)^{(\gamma - 7 + 12m)/4}, \tag{5}$$

where the relativistic particle index $\gamma = 1 - 2\alpha$, $\alpha = -1.08 \pm 0.08$ and expansion index $m = 0.86 \pm 0.02$. For SN 2008iz, $L \propto (\dot{M}/w)^{1.62}$. Consequently, for the radio emission to double its
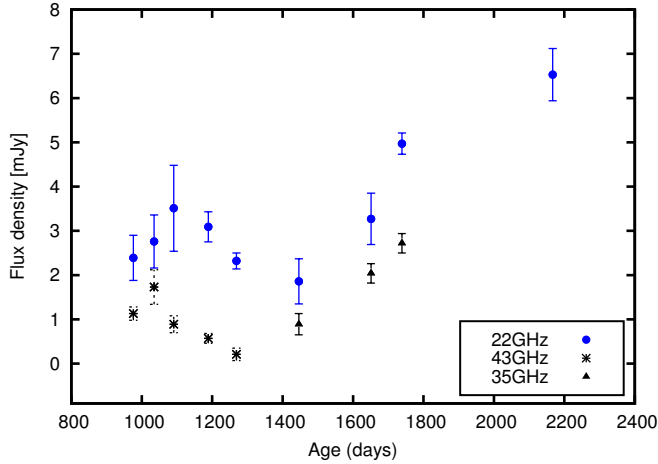
Fig. 8. Zoom into our higher frequency light-curve for a period between $t = 800$ to $t = 2400$ days. The flux density enhancement at $t \geq 1400$ days was detected in both VLA and VLBI results at all frequencies.

Fig. 9. Spectral index, α, for SN 2008iz obtained from fitting a simple power law fit to the radio continuum data at each epoch. The spectral index remains steep, near $\alpha = -1$.

flux in the first flare, the CSM density must have increased by a factor of 1.5, while for the increase by a factor of 4 in the second flare, the CSM density must have tripled. However, the VLBI images of the remnant of SN 2008iz do not show a spherically symmetric density enhancement. This suggests that the shock wave is encountering dense inhomogeneities in the CSM.

The late flare (day 1400) may also be related to the transition of the front shock from the CSM bubble into the ISM. This would enhance the magnetic field and increase the emission at all frequencies. However, we obtain that the size of the shock on day 1400 is ∼0.06 pc (3.6 mas), which is very small compared to the supernova remnant sizes measured by Batejat et al. (2011) of ∼0.4 pc in Arp 220 at the transition. If the flare were related to the transition, this would indicate a very dense ISM for the pressure balance to hold at the bubble boundary of SN 2008iz. Thus we require an ISM with a density higher than the characteristic one in Arp 220 of 10^4 cm^{-3} to explain the light curve of SN 2008iz at late stages, in the frame of the ISM interaction model.

4.2. Evolution of the spectral index

Figure 9 shows the best-fit radio spectral index, α, for SN 2008iz from ∼430 days up to 2167 days. To obtain the radio spectral index, we fit a simple power-law spectrum of the form ($S = S_0 \nu^\alpha$) to our VLA data for all the epochs except for epoch 2009 April 27, which was best fit with a broken power-law of the form

$$S = S_0 \left(\frac{\nu}{\nu_0}\right)^\alpha \left(1 - e^{-\left(\frac{\nu}{\nu_0}\right)^{\delta-\alpha}}\right) \quad (6)$$

as presented by Brunthaler et al. (2010). We fit this expression to our data and left S_0 and α as free parameters. For epochs with two or three frequency data points only, that is, 2010 October 20, 2010 December 18, 2011 July 30, and 2011 August 01, a systematic error of 30% was added to the fit error to account for the low data statistics. This causes the data points for these epochs to have slightly larger error bars than the epochs with more frequency data points, whose errors are derived directly from the post-fit covariance matrix. The observed spectral index does not show signs of evolution and remains steep, that is, $\alpha \sim -1$ throughout the period. This steepness seems to persist longer than for SN 1993J, whose spectral index evolution shows flattening at all frequencies beginning at an age
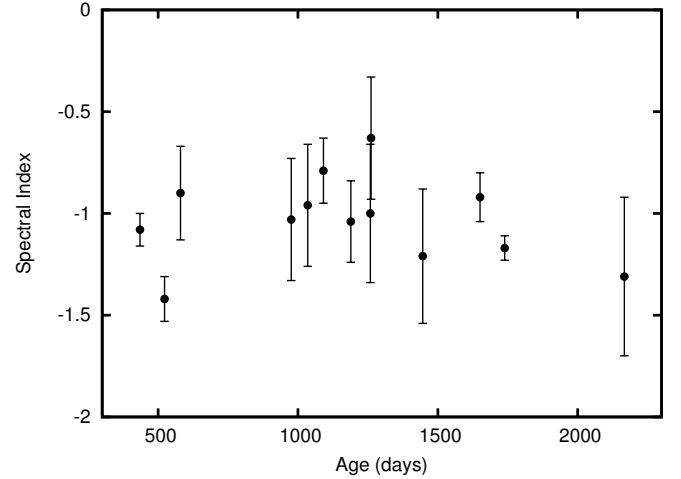
∼970 days (Pérez-Torres et al. 2002a; Martí-Vidal et al. 2011b; Weiler et al. 2007)

4.3. Equipartition, total minimum energy, and magnetic field

For sources of radio synchrotron emission, energy equipartition between the particles and the magnetic field is usually postulated (Pacholczyk 1970). The total minimum energy content ($E_{\min}$) and magnetic field (B_{eq}) in SN 2008iz can be expressed as described in relations 7 and 8

$$E_{\min} = c_{13}(1 + k)^{4/7}\phi^{3/7}R^{9/7}L^{4/7} \quad (7)$$

and

$$B_{\mathrm{eq}} = 4.5^{2/7}c_{12}^{2/7}(1 + k)^{2/7}\phi^{-2/7}R^{-6/7}L^{2/7}, \quad (8)$$

where the dimensionless parameters c_{12} and c_{13} are 9.3×10^7 and 3.3×10^4, respectively (Pacholczyk 1970) for a spectral index $\alpha \sim -1$. The filling factor, ϕ, the ratio of the inner and outer radii of the emitting region, is estimated as 0.3 (Marchili et al. 2010). R is the source radius in cm derived from our VLBI data $R_{50\%}$, which predicts $m = 0.86 \pm 0.02$ and $c_y = (7.5 \pm 0.9) \times 10^{-6}$ arcsec/day in agreement with previous derivations from Brunthaler et al. (2010) of $m = 0.89 \pm 0.03$. L is the integrated radio luminosity in erg^{-1} between the radio synchrotron cut-off frequencies $\nu_{\min} = 10^7$ Hz and $\nu_{\max} = 10^{11}$ Hz. k is the ratio between the relativistic heavy particle energy density to the relativistic electron energy density. The parameter k is dependent on masses of the particles and varies from $m_{\mathrm{p}}/m_{\mathrm{e}} \approx 1$ to $m_{\mathrm{p}}/m_{\mathrm{e}} \approx 2 \times 10^3$ (Marchili et al. 2010). With a varying value of k, we cannot compute a single value of the total minimum energy and equipartition magnetic field, but can only give a range of possibilities (see Table 1). The derived $E_{\min}$ values are in the range of ∼10^{46}–∼10^{48} erg. Our results of B_{eq} at 2008 May 3, which range between 0.25 G and 1.78 G, are comparable to the values derived by Marchili et al. (2010) at 5 GHz of 0.3 G and 2.1 G and also on 2009 April 8 between 0.04 G and 0.27 G, compared to 0.04 G and 0.31 G, respectively. Figure 10 shows the magnetic field evolution as the supernova ages derived from the integrated 22.3 GHz flux densities from day ∼36 to ∼2200 after the explosion. From this figure, we note that the magnetic fields at each epoch scale with time, showing a hint of flattening at the

Table 1. SN 2008iz derived equipartition total minimum energy and magnetic fields.

Date (yy/mm/dd)	Days since 18-2-2008	Radius (cm)	Luminosity (erg^{-1})	B_{eq} (G)$_{k=1}$	B_{eq} (G)$_{k=2000}$	E_{min} (erg)$_{k=1}$	E_{min} (erg)$_{k=2000}$
2008/03/24	36	0.88×10^{16}	142.6×10^{35}	0.444	3.197	1.58×10^{46}	0.82×10^{48}
2008/05/03	76	1.67×10^{16}	126.6×10^{35}	0.248	1.784	3.35×10^{46}	1.74×10^{48}
2009/04/08	416	7.22×10^{16}	13.2×10^{35}	0.037	0.266	6.05×10^{46}	3.14×10^{48}
2009/04/27	435	7.51×10^{16}	8.9×10^{35}	0.032	0.230	5.08×10^{46}	2.63×10^{48}
2009/09/19	580	9.61×10^{16}	6.5×10^{35}	0.024	0.170	5.83×10^{46}	3.02×10^{48}
2009/10/21	612	10.07×10^{16}	4.4×10^{35}	0.020	0.146	4.96×10^{46}	2.57×10^{48}
2010/10/20	976	15.04×10^{16}	3.4×10^{35}	0.013	0.096	7.16×10^{46}	3.71×10^{48}
2010/12/18	1035	15.82×10^{16}	4.0×10^{35}	0.013	0.097	8.39×10^{46}	4.35×10^{48}
2011/02/12	1091	16.55×10^{16}	5.0×10^{35}	0.014	0.099	10.10×10^{46}	5.23×10^{48}
2011/05/21	1189	17.82×10^{16}	4.4×10^{35}	0.012	0.090	10.32×10^{46}	5.35×10^{48}
2011/08/09	1269	18.85×10^{16}	3.3×10^{35}	0.011	0.079	9.42×10^{46}	4.88×10^{48}
2012/02/02	1446	21.09×10^{16}	2.7×10^{35}	0.009	0.068	9.70×10^{46}	5.03×10^{48}
2012/08/25	1651	23.64×10^{16}	4.7×10^{35}	0.010	0.072	15.42×10^{46}	7.99×10^{48}
2012/11/21	1739	24.72×10^{16}	7.1×10^{35}	0.011	0.078	20.67×10^{46}	10.71×10^{48}
2014/01/23	2167	29.90×10^{16}	9.1×10^{35}	0.010	0.071	30.23×10^{46}	15.66×10^{48}

Notes. The luminosity is derived from the 22.3 GHz integrated flux values, while the radius is derived from the VLBI results by assuming a constant expansion index $m = 0.86 \pm 0.02$ and $c_y = (7.5 \pm 0.9) \times 10^{-6}$ arcsec/day.

time $\geq$ day 1300. This flattening corresponds to the flux-density flare events when the shock interacts with dense CSM. However, assuming a constant k value, the magnetic field generally decreases according to $B \propto t^{-1}$ in the full time range.

Considering the equipartition between fields and particles, the B_{eq} range between $(37-266)$ mG on 2009 April 8 (day 416) is expected to explain the observed level of radio emission. The choice of the radius, which is $\sim 7.2 \times 10^{16}$ cm, allows for a comparison with other supernovae at about the same point of expansion. The energy density of the magnetic field in the remnant is postulated to be lower than the kinetic energy density (i.e. $\rho_{csm} v_{csm}^2 / 2 \gtrsim B_{csm}^2 / 8\pi$), such that

$$B_{csm} \lesssim \frac{(\dot{M} v_w)^{1/2}}{r}$$
$$= 2.5 \left(\frac{\dot{M}}{10^{-5} M_\odot \, yr^{-1}} \right)^{1/2} \left(\frac{v_w}{10 \, km \, s^{-1}} \right)^{1/2} \left(\frac{r}{10^{16} \, cm} \right)^{-1} mG. \tag{9}$$

Using a mass-loss of the progenitor of SN 2008iz of $\sim 3.69 \times 10^{-5} \, M_\odot \, yr^{-1}$ (Marchili et al. 2010), a standard pre-supernova wind velocity v_w of 10 km s^{-1}, and a standard CSM density profile of $\rho_{wind} \propto r^{-2}$, we obtain $B_{csm} = 0.67$ mG, which is a factor of about $55-400$ times smaller than the equipartition field. This indicates that the magnetic field inferred for SN 2008iz cannot originate solely from compression of the existing circumstellar magnetic field, which is predicted to increase the field only by a factor of 4 (Dyson & Williams 1980). Large amplification factors of the magnetic field have also been found for other radio supernova: for SN 2001gd an amplification factor in the range of $50-350$ was determined (Pérez-Torres et al. 2005); the SN 1993J amplification factor of a few hundred (Fransson & Björnsson 1998; Pérez-Torres et al. 2001); for SN 1986J values in the range of $40-300$ (Pérez-Torres et al. 2002b); for SN 1979C in the range of $50-400$ (Pérez-Torres et al. 2005); and between 37 and 260 for SN 2004et (Martí-Vidal et al. 2007). Thus, if equipartition between fields and particles holds, amplification mechanisms other than compression of the circumstellar
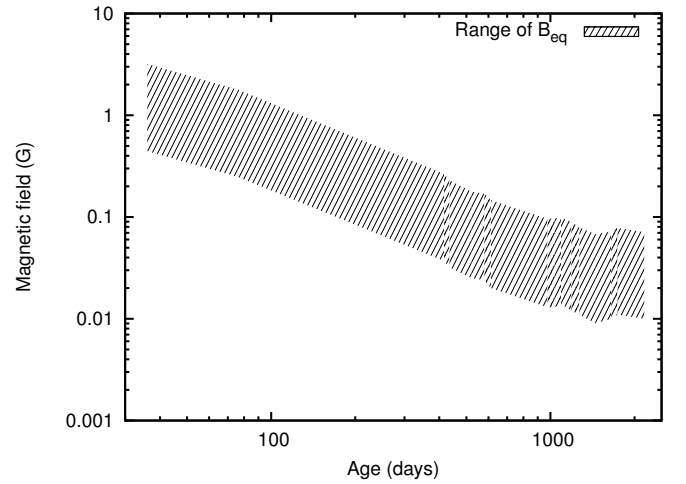

Fig. 10. 22 GHz evolution of the magnetic field in the synchrotron-emitting plasma of SN 2008iz with time. The magnetic field evolution is roughly consistent with $B \propto t^{-1}$ with signs of flattening past day $\sim$970.

magnetic field need to be invoked to explain the level of radio emission from the supernova, such as turbulent amplification due to Rayleigh-Taylor instability (Chevalier 1982; Chevalier & Blondin 1995).

5. Summary

We reported on multi-frequency VLA and VLBI radio data in the optically thin regime for an on-going monitoring campaign of SN 2008iz. We fitted two models to the data, a simple power-law ($S \propto t^\beta$) and a simplified Weiler model, yielding $\beta = -1.22 \pm 0.07$ (days $100-1500$) and -1.41 ± 0.02 (days $76-2167$), respectively. The light curve uncovers flux density enhancements at $t = 970$ days and $t = 1400$ days by a factor of $\sim$2 and $\sim$4, respectively. The later flare, except for being brighter, does not show signs of decline, at least from the results

examined so far (2014 January 23; day 2167). The flaring activity is attributed to increase in the number density of shocked circumstellar medium (CSM) electrons as the expanding shock wave encounters a clumpy denser medium. The late flare may also be attributed to the transition of the front shock from the CSM bubble into the interstellar medium (ISM), although a very dense ISM ($>10^4$ cm^{-3}) would be required, which is consistent with SN 2008iz being deeply buried within the centre of M 82.

The 1.4 GHz flux density values fall below the supernova model fit, a phenomenon confirmed by the 3σ LOFAR non-detection limit at 154 MHz level of 0.41 mJy/beam. The low flux values could be attributed to free-free absorption (FFA) from a dense foreground screen along the line of sight, or a low-frequency cut-off caused by the Razin-Tsytovich effect.

The spectrum for SN 2008iz for the period from ∼430 to 2167 days after the supernova explosion shows no signs of evolution and remains steep ($\alpha \sim -1$). This is different from SN 1993J, whose spectral index evolution shows α flattening of the spectrum at all frequencies, beginning at an age ∼970 days.

From the 4.8 and 8.4 GHz VLBI images, the supernova expansion is seen to start with a shell-like structure, reflecting an expansion with similar velocities into all directions that becomes increasingly more asymmetric at later stages. Finally, in later epochs the structure breaks up, with bright structures dominating the lower part of the ring, which serves as an indication of a denser surrounding medium along the southern direction. This structural evolution differs significantly from SN 1993J, which remains circularly symmetric over 4000 days after the explosion. From the size evolution of the SN 2008iz SNR derived from the 4.8 and 8.4 GHz VLBI images, a deceleration parameter, m, of 0.86 ± 0.02 and an expansion velocity of $(12.1 \pm 0.2) \times 10^3$ km s^{-1} are derived for the time range between 73 and 1400 days.

From the energy equipartition between fields and particles, we estimate the minimum total energy in relativistic particles and the magnetic fields during the supernova expansion. On 2009 April 8, $E_{min} \propto 3.15 \times 10^{46} - 1.63 \times 10^{48}$ erg, which corresponds to an average equipartition magnetic field of $B_{min} \propto 37-266$ mG. We derive the average magnetic field in the circumstellar wind of $B_{csm} = 0.67$ mG at a radius from the centre of the supernova explosion of ∼7.2×10^{16} cm. Since the supernova shock compression could only enhance the magnetic field by a factor of 4, powerful amplification mechanisms must be at play in SN 2008iz to account for the derived magnetic field amplification of $55-400$ that is responsible for the synchrotron radio emission.

References

Batejat, F., Conway, J. E., Hurley, R., et al. 2011, ApJ, 740, 95
Beswick, R. J., Riley, J. D., Marti-Vidal, I., et al. 2006, MNRAS, 369, 1221
Beswick, R. J., Muxlow, T. W. B., Pedlar, A., et al. 2009, ATel, 2060
Brunthaler, A., Menten, K. M., Reid, M. J., et al. 2009a, ATel, 2020
Brunthaler, A., Menten, K. M., Reid, M. J., et al. 2009b, A&A, 499, L17
Brunthaler, A., Martí-Vidal, I., Menten, K. M., et al. 2010, A&A, 516, A27
Chevalier, R. A. 1982, ApJ, 258, 790
Chevalier, R., & Blondin, J. M. 1995, ApJ, 444, 312
Deller, A. T., Brisken, W. F., Phillips, C. J., et al. 2011, PASP, 123, 275
Dyson, J., & Williams, D. 1980, Physics of the Interstellar Medium (Manchester: Manchester University Press)
Fenech, D. M., Muxlow, T. W. B., Beswick, R. J., Pedlar, A., & Argo, M. K. 2008, MNRAS, 391, 1384
Fransson, C., & Björnsson, C.-I. 1998, ApJ, 509, 861
Freedman, W. L., Hughes, S. M., Madore, B. F., et al. 1994, ApJ, 427, 628
Güver, T., & Özel, F. 2009, MNRAS, 400, 2050
Kronberg, P. P., Sramek, R. A., Birk, G. T., et al. 2000, ApJ, 535, 706
Marcaide, J. M., Alberdi, A., Ros, E., et al. 1997, ApJ, 486, L31
Marchili, N., Martí-Vidal, I., Brunthaler, A., et al. 2010, A&A, 509, A47
Martí-Vidal, I., Marcaide, J. M., Alberdi, A., et al. 2007, A&A, 470, 1071
Martí-Vidal, I., Marcaide, J. M., Alberdi, A., et al. 2011a, A&A, 526, A142
Martí-Vidal, I., Marcaide, J. M., Alberdi, A., et al. 2011b, A&A, 526, A143
Mattila, S., Fraser, M., Smartt, S. J., et al. 2013, MNRAS, 431, 2050
Muxlow, T. W. B., Pedlar, A., Wilkinson, P. N., et al. 1994, MNRAS, 266, 455
Muxlow, T. W. B., Beswick, R. J., Pedlar, A., et al. 2009, ATel, 2073
Pacholczyk, A. G. 1970, Radio astrophysics. Nonthermal processes in galactic and extragalactic sources (San Francisco: Freeman Publishers)
Pérez-Torres, M. A., Alberdi, A., & Marcaide, J. M. 2001, A&A, 374, 997
Pérez-Torres, M. A., Alberdi, A., & Marcaide, J. M. 2002a, A&A, 394, 71
Pérez-Torres, M. A., Alberdi, A., Marcaide, J. M., et al. 2002b, MNRAS, 335, L23
Pérez-Torres, M. A., Alberdi, A., Marcaide, J. M., et al. 2005, MNRAS, 360, 1055
Pérez-Torres, M. A., Lundqvist, P., Beswick, R. J., et al. 2014, ApJ, 792, 38
van Dyk, S. D., Weiler, K. W., Sramek, R. A., Rupen, M. P., & Panagia, N. 1994, ApJ, 432, L115
Varenius, E., Conway, J. E., Martí-Vidal, I., et al. 2015, A&A, 574, A114
Weiler, K. W., Panagia, N., Montes, M. J., & Sramek, R. A. 2002, ARA&A, 40, 387
Weiler, K. W., Williams, C. L., Panagia, N., et al. 2007, ApJ, 671, 1959
Weiß, A., Neininger, N., Hüttemeister, S., & Klein, U. 2001, A&A, 365, 571

Appendix A: Additional tables

Table A.1. Log of SN 2008iz integrated radio flux measurements observed with VLA.

Date (dd/mm/yy)	Days since 18-2-2008	Configuration	$S_{1.4\,\mathrm{GHz}}$ (mJy)	$S_{4.8\,\mathrm{GHz}}$ (mJy)	$S_{8.4\,\mathrm{GHz}}$ (mJy)	$S_{22.3\,\mathrm{GHz}}$ (mJy)	$S_{35\,\mathrm{GHz}}$ (mJy)	$S_{43.2\,\mathrm{GHz}}$ (mJy)
2008/03/24	36	C	–	–	–	100 ± 2	–	–
2008/05/03	76	C	–	–	–	88.4 ± 0.2	–	–
2009/04/08	416	B	–	–	–	9.2 ± 0.2	–	–
2009/04/27	435	B	55 ± 6	30 ± 5	14 ± 3	6.2 ± 0.7	–	2.5 ± 0.4
2009/07/24	523	C	–	21 ± 2	11 ± 1	–	–	1.0 ± 0.6
2009/09/19	580	B	–	14 ± 2	6 ± 2	5 ± 2	–	1.8 ± 0.5
2009/10/21	612	D	–	–	–	3 ± 1	–	–
2010/10/20	976	C	–	–	–	2.4 ± 0.3	–	1.1 ± 0.2
2010/12/18	1035	C	–	–	10.1 ± 0.9	2.8 ± 0.3	–	1.7 ± 0.4
2011/02/12	1091	B	–	10.2 ± 0.6	7.7 ± 0.7	3.5 ± 0.1	–	0.9 ± 0.2
2011/05/21	1189	AB	23 ± 5	6 ± 2	6.4 ± 0.7	3.1 ± 0.3	–	0.6 ± 0.1
2011/07/30	1259	A	19 ± 3	12.3 ± 0.9	7.5 ± 0.5	–	–	–
2011/08/01	1261	A	17 ± 2	11 ± 1	7.1 ± 0.4	–	–	–
2011/08/09	1269	A	–	–	–	2.3 ± 0.2	–	0.2 ± 0.1
2012/02/02	1446	C	–	–	–	1.9 ± 0.5	0.9 ± 0.2	–
2012/08/25	1651	B	–	12 ± 2	9 ± 2	3.3 ± 0.6	2.0 ± 0.2	–
2012/11/21	1739	A	–	26 ± 1	16.8 ± 0.9	5.0 ± 0.2	2.7 ± 0.2	–
2014/01/23	2167	AB	–	41 ± 7	–	6.5 ± 0.6	–	–

Notes. The data on days 24 Mar 2008 to 27 Apr 2009 are obtained from Brunthaler et al. (2009b) and Brunthaler et al. (2010).

Table A.2. Log of SN 2008iz radio flux and angular size measurements obtained from the VLBI observations.

Date	Age $(t - t_0)$	$S_{1.6\,\mathrm{GHz}}$ (mJy)	$S_{1.6\,\mathrm{GHz}}$ (mJy/b)	$S_{4.8\,\mathrm{GHz}}$ (mJy/b)	$S_{8.4\,\mathrm{GHz}}$ (mJy/b)	$\Theta_{R_{50\%}\,4.8\,\mathrm{GHz}}$ (mas)	$\Theta_{R_{50\%}\,8.4\,\mathrm{GHz}}$ (mas)
2009/10/04	595	64 ± 6	57.9 ± 0.5	3.02 ± 0.04	0.83 ± 0.04	1.8 ± 0.2	1.7 ± 0.2
2009/12/04	656	55 ± 4	50.9 ± 0.4	2.61 ± 0.03	0.78 ± 0.03	1.9 ± 0.2	1.8 ± 0.1
2010/02/06	720	42 ± 8	34.6 ± 0.2	2.09 ± 0.03	0.59 ± 0.03	2.0 ± 0.2	2.0 ± 0.1
2010/03/20	758	–	–	1.80 ± 0.03	–	2.3 ± 0.2	–
2010/05/04	807	39 ± 9	30.8 ± 0.2	1.79 ± 0.03	0.58 ± 0.03	2.3 ± 0.2	2.2 ± 0.1
2010/05/29	828	–	–	1.71 ± 0.03	–	2.4 ± 0.2	–
2010/06/07	840	32 ± 8	24.9 ± 0.1	–	–	–	–
2010/07/02	866	35 ± 8	26.5 ± 0.2	4.56 ± 0.05	1.34 ± 0.05	–	2.4 ± 0.2
2010/09/05	931	30 ± 9	20.8 ± 0.1	3.73 ± 0.04	0.56 ± 0.03	2.5 ± 0.2	2.5 ± 0.2
2010/11/19	1006	30 ± 9	21.5 ± 0.1	1.73 ± 0.03	0.41 ± 0.03	2.8 ± 0.2	2.8 ± 0.2
2011/01/07	1055	27 ± 9	17.6 ± 0.1	1.15 ± 0.03	1.02 ± 0.05	2.9 ± 0.3	2.8 ± 0.2
2011/03/18	1125	26 ± 9	17.1 ± 0.1	0.98 ± 0.03	0.41 ± 0.03	3.0 ± 0.3	3.0 ± 0.2
2011/05/12	1180	26 ± 9	17.3 ± 0.2	0.76 ± 0.03	0.33 ± 0.02	3.1 ± 0.3	3.0 ± 0.2
2011/08/14	1274	25 ± 10	15.2 ± 0.1	1.55 ± 0.05	0.57 ± 0.04	–	3.2 ± 0.2
2011/08/14	1274	24 ± 9	15.3 ± 0.1	3.78 ± 0.04	1.18 ± 0.04	–	–
2011/09/23	1314	25 ± 2	12.6 ± 0.1	0.91 ± 0.03	0.29 ± 0.03	3.4 ± 0.3	3.3 ± 0.2
2011/09/23	1314	21 ± 9	12.0 ± 0.1	3.17 ± 0.07	0.90 ± 0.03	–	3.3 ± 0.2
2011/12/19	1401	28 ± 9	18.7 ± 0.2	0.75 ± 0.03	0.35 ± 0.03	3.7 ± 0.6	3.7 ± 0.3
2012/08/25	1650	39 ± 9	30.3 ± 0.3	2.43 ± 0.05	0.73 ± 0.03	4.3 ± 0.4	4.5 ± 0.2
2013/01/28	1806	40 ± 9	21.2 ± 0.1	1.65 ± 0.01	0.69 ± 0.01	8.0 ± 0.4	4.9 ± 0.2

Notes. Both peak and integrated flux density values of our 1.6 GHz are displayed. The peak flux values are presented for the 4.8 GHz and 8.4 GHz measurements because the supernova SN 2008iz was resolved at these frequencies. The $\Theta_{R_{50\%}}$ are the angular sizes derived as the radius of the supernova ring at 50% of the peak intensity on the outside of the bright rim.